in vivo *26*: 671-682 (2012)

Sorafenib Inhibits TPA-Induced MMP-9 and VEGF Expression *via* Suppression of ERK/NF-κB Pathway in Hepatocellular Carcinoma Cells

I.-TSANG CHIANG[1*], YU-CHANG LIU[1,2*], WEI-HSUN WANG[1,3*], FEI-TING HSU[1], HONG-WEN CHEN[4], WUU-JYH LIN[5], WEN-YI CHANG[1] and JENG-JONG HWANG[1]

[1]*Department of Biomedical Imaging and Radiological Sciences, National Yang-Ming University, Taipei, Taiwan, R.O.C.;*
[2]*Department of Radiation Oncology, National Yang-Ming University Hospital, Yilan, Taiwan, R.O.C.;*
[3]*Department of Orthopedic Surgery, Changhua Christian Hospital, Changhua, Taiwan, R.O.C.;*
[4]*Department of Radiation Oncology and Hospice Care Center, Mackay Memorial Hospital, Taipei, Taiwan, R.O.C.;*
[5]*Division of Radioisotope, Institute of Nuclear Energy Research, Taoyuan, Taiwan, R.O.C.*

Abstract. *Invasion by hepatocellular carcinoma (HCC) has been reported to occur via the up-regulation of nuclear factor-kappaB (NF-κB). Sorafenib can improve the overall survival in patients with HCC, however, the association of its inhibitory mechanisms with the inactivation of NF-κB remains unclear. Here, Huh7 cell line transfected with NF-κB-luc2 vector was used to study the effects of sorafenib on NF-κB activity, on expressions of matrix metalloproteinase-9 (MMP-9) and vascular endothelial growth factor (VEGF), which were induced by 12-O-tetradecanoylphorbol-13-acetate (TPA). TPA increased the NF-κB activity and the expressions of MMP-9 and VEGF significantly, but its effects were suppressed by sorafenib in a dose-dependent manner. Similar results were found with PD98059, an inhibitor of extracellular signal-regulated kinase (ERK). Furthermore, transfection of Huh7 cell with an inhibitor of kappaB-α mutant vector, led to reduced TPA-induced MMP-9 and VEGF mRNA expressions. Sorafenib inhibits TPA-induced MMP-9 and VEGF expressions via the suppression of ERK/NF-κB pathway in HCC cells.*

Hepatocellular carcinoma (HCC) is ranked fourth regarding cancer-related mortality worldwide (1). The prognosis of HCC is generally poor, mainly due to the invasion of liver vessels and distant metastases (2). Degradation of the extracellular matrix (ECM) and basement membrane are the key steps for cancer cells to initiate the invasion process (3). Matrix metalloproteinases (MMPs) are a family of ECM-degrading enzymes, and may augment the tumor invasiveness and metastasis, with MMP-9 playing a crucial role (4). Increased microvessel density is associated with a poor outcome after surgery, and correlates well with the risk for vascular invasion, metastasis, and worse disease-free interval (5). Vascular endothelial growth factor (VEGF) is the principal mediator of angiogenesis, and VEGF is usually found overexpressed in HCC (2, 6). Furthermore, high VEGF expression has been shown to be associated with poor survival in HCC (2).

HCC usually develops in patients with chronic hepatitis, in which nuclear factor-kappaB (NF-κB) provides a mechanistic link between chronic inflammation and liver cancer initiation (7, 8). NF-κB is a key molecule responsible not only for pre-malignant and malignant cells to escape apoptosis-based tumor surveillance (9, 10), but for the development and progression of HCC (7, 11). NF-κB is also involved in the regulation of angiogenesis and invasiveness in HCC (12, 13). NF-κB-regulated down-stream genes, such

*These Authors contributed equally to this study.

Abbreviations: BLI: Bioluminescent imaging; EMSA: electrophoretic mobility shift assay; p-ERK: phosphorylated extracellular signal-regulated kinase; T-ERK: total extracellular signal-regulated kinase; IκB: inhibitor of kappaB; IκBαM: dominant negative mutant construct of IκB-α; IKK: IκB kinase; MMP-9: matrix metalloproteinase-9; MTT: 3-(4,5-Dimethylthiazol-2-yl)-2,5-diphenyltetrazolium bromide; RT-PCR: reverse transcription polymerase chain reaction; SD: standard deviation; TPA: 12-O-tetradecanoylphorbol-13-acetate; VEGF: vascular endothelial growth factor.

Correspondence to: Jeng-Jong Hwang, Department of Biomedical Imaging and Radiological Sciences, National Yang-Ming University, No. 155, Sec. 2, Li-Nong St., Bei-tou, Taipei 112, Taiwan, R.O.C. Tel: +886 228267064, Fax: +886 228201095, e-mail: jjhwang@ym.edu.tw

Key Words: Hepatocellular carcinoma, sorafenib, NF-κB, MMP-9, VEGF, Huh 7 cells.

as those encoding pro-inflammatory cytokines, adhesion molecules, angiogenic factors and ECM degradation enzymes, are associated with tumor progression (14). NF-κB/Rel dimer is generally sequestered in the cytoplasm by inhibitor of kappaB (IκB), which binds with high affinity to p65 (RelA) of the NF-κB family. In order to activate the NF-κB signaling pathway, IκB needs to be phosphorylated by IκB kinase (IKK) to release the bound NF-κB/Rel dimer for subsequent nuclear translocation, in order to regulate down-stream genes in HCC (12, 15). Therefore, IKK may be a good target for inhibition of NF-κB signaling (16). On the other hand, the RAF/mitogen-activated protein kinase kinase (MEK)/extracellular signal-regulated kinase (ERK) signaling cascade is another pathway responsible for development of HCC (17). Sorafenib (BAY 43-9006, Nexavar®, Bayer Inc., Leverkusen, North Rhine-Westphalia, Germany) is a multi-kinase inhibitor against RAF kinase and several receptor tyrosine kinases (RTKs), including VEGF receptor 2 and 3 (VEGFR2/3), platelet-derived growth factor receptor (PDGFR), Feline sarcoma virus-strain McDonough (FMS)-like tyrosine kinase 3 (FLT3), rearranged during transfection (RET), and Mast/stem cell growth factor receptor (c-KIT) (18-20). It has been shown, in a phase III clinical trail and by the US FDA, that sorafenib prolongs the survival of patients with advanced HCC for months (21). Malignant transformation of rat liver epithelial cells is mediated through RAS/RAF/NF-κB pathway, which can be reversed by the inhibition of IKK-α (22). Inhibition of NF-κB reduces the invasion and angiogenesis *via* the suppression of MMP-9 and VEGF expressions in HCC (12). Nevertheless, whether sorafenib can inhibit the invasion and angiogenesis through the inactivation of NF-κB and its regulated down-stream genes in HCC, remains unclear. 12-*O*-Tetradecanoylphorbol-13-acetate (TPA), a promoter for malignant formation, has been reported to have the capability to induce the invasiveness of tumor cells through NF-κB activity and the subsequent MMP-9 and VEGF expressions, in HCC and other tumor cell lines (23-25).

Bioluminescent imaging (BLI) with NF-κB-driven luciferase gene is a rapid and non-invasive biotechnological tool for screening drugs with anti-NF-κB effects both *in vitro* and *in vivo* (16). Here, we investigated the effects of sorafenib on NF-κB activity, and the expressions of its regulated down-stream proteins, mainly MMP-9 and VEGF, in HCC using TPA as the inducer. Investigations were assayed with BLI and other biotechnological tools.

Materials and Methods

Cell culture. Huh7 cell line was provided kindly by Dr. Chia-Hsien Cheng at the Department of Radiation Oncology, National Taiwan University Hospital, Taipei, Taiwan, and maintained in Dulbecco's modified Eagle's medium (DMEM) supplemented with 10% fetal bovine serum (FBS). All cultures were maintained at 37˚C in a humidified incubator containing 5% CO_2. The Huh7/NF-κB-*luc2* stable clone was maintained in the same condition except 500 μg/ml G418 (Calbiochem, Darmstadt, Hesse, Germany) was added.

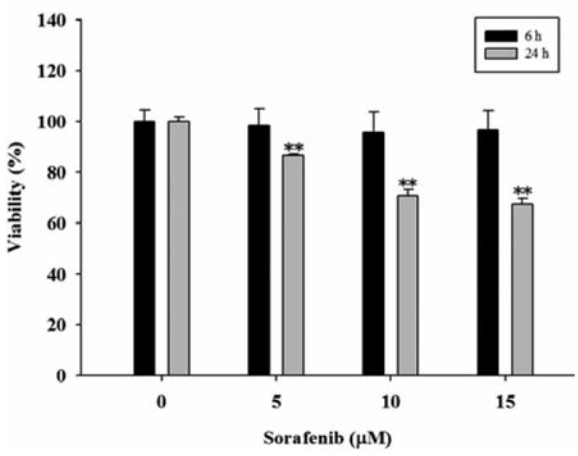

Figure 1. *Cytotoxicity of sorafenib on Huh7/NF-κB-luc2 cells occurs in a dose-dependent manner. Cells were treated with 0-15 μM sorafenib for 6 and 24 h, respectively. Cell viability was determined by the 3-(4,5-Dimethylthiazol-2-yl)-2,5-diphenyltetrazolium bromide (MTT) assay. Data are presented as means±SD (n=3). **p<0.01 as compared with that of dimethyl sulfoxide (DMSO)-treated control. The experiments were repeated three times.*

Construction of NF-κB/luc2 vector. Standard cloning technique was used to insert the NF-κB-responsive element into a pGL4-*luc2* vector (Promega, Madison, WI, USA). pGL4-*luc2* was digested with *Ase*I and *Bsa*I, then blunted with Klenow enzyme. The NF-κB-responsive elements were isolated from pNF-κB-luc vector (Clontech, Mountain View, CA, USA) by *Mlu*I and *Hind*III, and then blunted with Klenow enzyme. The NF-κB-responsive element was inserted and ligated into digested pGL4-*luc2*, resulting in a pNF-κB-luc2 vector.

Plasmid transfection and stable clone selection. The transfection of Huh7 was performed using jetPEI™ (Polyplus Transfection, New York, NY, USA). 2×10^6 cells were seeded in a 100-mm diameter dish 24 h before transfection. Both 8 μg of pNF-κB-*luc2* vector DNA and 16 μl of jetPEI™ solution were diluted into 500 μl of 145 μM NaCl, respectively, then immediately mixed together, and incubated for 30 min at room temperature. The jetPEI™/DNA mixture was added to the cells in the 100-mm dish, which was then incubated at 37˚C for 24 h. Cells were then trypsinized and cultured with DMEM containing 1 mg/ml G418, supplemented with 10% FBS for two weeks. The surviving clones were isolated, and transferred to 96-well plates for growth. The Luc2 protein expression in each clone was assayed using BLI. The recombinant bioluminescent cell clone was renamed as Huh7/NF-κB-*luc2* cell line. IκBα mutant vector (p-IκBαM, Clontech, Mountain View, CA, USA) was used to transfect Huh7/NF-κB-*luc2* cells with the same protocol as described previously. The inhibitory effects of p-IκBαM super repressor on NF-κB activity was confirmed with BLI and electrophoretic mobility shift assay (EMSA) and was used as a negative control.

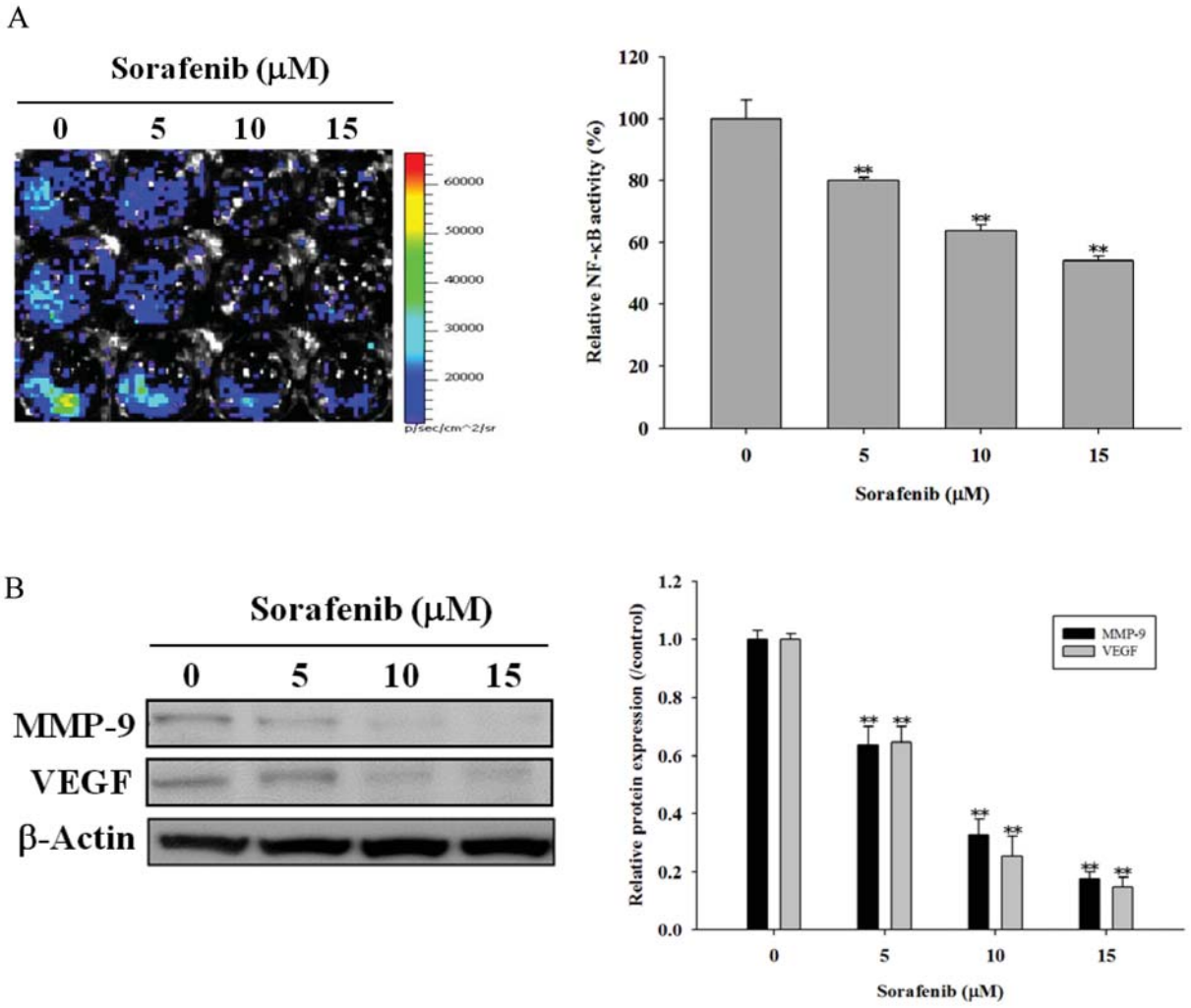

Figure 2. *Intrinsic nuclear factor kappaB (NF-κB) activity, matrix metalloproteinase-9 (MMP-9) and vascular endothelial growth factor (VEGF) expressions are inhibited by sorafenib in a dose-dependent manner in Huh7/NF-κB-luc2 cells. Cells were incubated with different concentration of sorafenib for 6 hours. A: Left: Bioluminescent imaging (BLI) of the relative NF-κB activity versus the concentration of sorafenib; right: quantification of the relative NF-κB activity. B: Top: Western blotting of MMP-9 and VEGF expressions using β-actin as the internal control; bottom: quantification of the western blotting. The ratios of MMP-9/β-actin and VEGF/β-actin in sorafenib-treated groups are compared with those of the dimethyl sulfoxide (DMSO)-treated control. Data are presented as means±SD (n=3). **p<0.01 as compared with that of DMSO-treated control. The experiments were repeated three times.*

Extraction of sorafenib from Nexavar® tablets. Extraction of sorafenib from commercial Nexavar® tablets was described in our previous study (26). In brief, a Nexavar® tablet, composed of 200 mg sorafenib, was ground to fine powder and transferred to a 100 ml conical flask. The powder was washed with 15 ml deionized distilled water three times to remove water-soluble components; 15 ml ethyl acetate was then used to extract the precipitate three times in order to recover the sorafenib. The organic phases were combined and dried over anhydrous sodium sulfate, followed by evaporation under reduced pressure. The residue was recrystallized with acetone and hexane to yield a white solid, which weighed about 122 mg (60% recovery). Nuclear magnetic resonance (NMR) spectra were recorded with a spectrometer (Varian Gemini 200; Oxford Instruments, Abingdon, Oxfordshire, UK) to determine the chemical structure of the sorafenib extract. High-performance liquid chromatography (HPLC) was conducted using a PU-2089 plus quaternary gradient pump (Jasco, Tokyo, Japan), equipped with a UV-2075 Plus intelligent UV/VIS detector (Jasco, Tokyo, Japan). The ^{1}H-NMR spectrum of the recovered sorafenib was the same as the one reported by Bankston *et al*. (27). Greater than 98% chemical purity, as determined with HPLC, was achieved for the recovered sorafenib (retention time=16.2 minutes).

3-(4,5-Dimethylthiazol-2-yl)-2,5-diphenyltetrazolium bromide (MTT) assay. MTT (Sigma-Aldrich, St. Louis, MO, USA) was dissolved in phosphate-buffered saline (145 mM NaCl, 1.4 mM KH_2PO_4, 4.3 mM Na_2HPO_4, and 2.7 mM KCl, pH 7.2). Huh7/NF-κB-*luc2* cells were seeded into 96-well plates at a density of 3×10^4 cells/well and were cultured for 24 h before treatment with different concentrations of sorafenib [0, 5, 10, and 15 μM in 0.1% dimethyl sulfoxide (DMSO)]

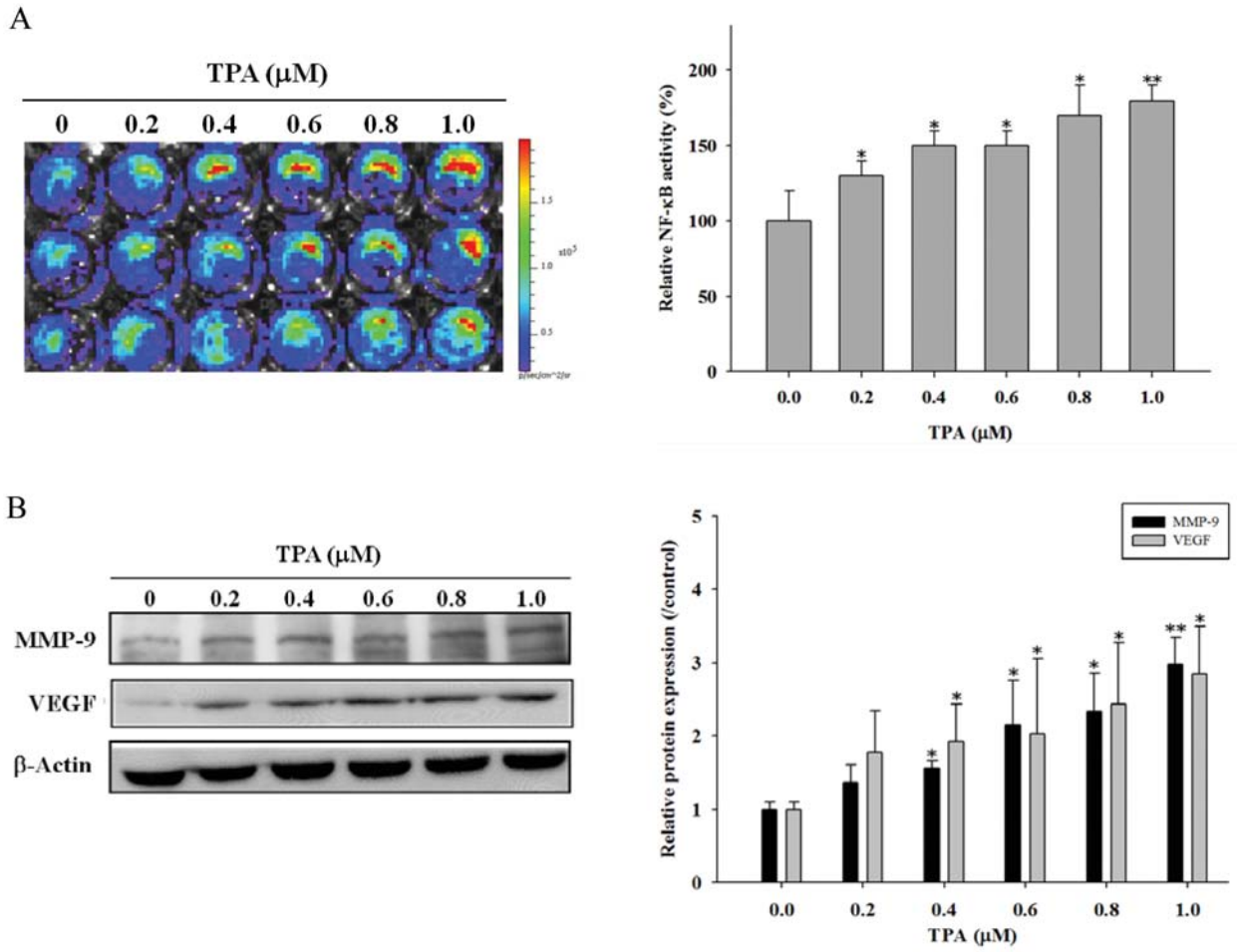

Figure 3. *Intrinsic nuclear factor kappaB (NF-κB) activity, matrix metalloproteinase-9 (MMP-9) and vascular endothelial growth factor (VEGF) expressions are increased by 12-O-tetradecanoylphorbol-13-acetate (TPA) in a dose-dependent manner in Huh7/NF-κB-luc2 cells. Cells were incubated with various concentrations of TPA for 6 hours. A: Top: Bioluminescent imaging (BLI) of the relative NF-κB activity versus the concentration of TPA; bottom: quantification of the relative NF-κB activity. B: Top: Western blotting of MMP-9 and VEGF expressions using β-actin as the internal control; bottom: quantification of the western blotting. Data are presented as means±SD (n=3). *p<0.05, **p<0.01 as compared with that of dimethyl sulfoxide (DMSO)-treated control. The experiments were repeated three times.*

for an additional 6 and 24 h, respectively. After washing with fresh medium, 100 μl of 5 mg/ml MTT solution was added to each well. After 2 h incubation at 37˚C, 100 μl DMSO were added to dissolve the MTT formazan product and the absorbance was determined with an ELISA reader (Power Wave ×340; Bio-Tek Instrument Inc., Winooski, VT, USA) using a wavelength of 570 nm for excitation.

NF-κB luciferase reporter gene assay. Huh7/NF-κB-luc2 cells, 3×10^4/well were cultured in a 96-well plate for 24 h, and then treated with sorafenib, TPA, and sorafenib or PD98059, 30 min prior to the addition of TPA, respectively, for 6 h. One hundred microliters of 500 μM D-luciferin (Xenogen, Hopkinton, MA, USA) were added to each well, and images were acquired for 1 min using an IVIS50 Imaging System (Xenogen, Hopkinton, MA, USA). Signals were quantified as photons/second, and compared with that of the DMSO-treated control to obtain the relative NF-κB activity with the Living Image software (Xenogen, Hopkinton, MA, USA).

Western blotting. Huh7/NF-κB-*luc2* cells, 2×10^6 were seeded into 100-mm diameter dishes for 24 hours, and then treated with sorafenib, TPA, combination of sorafenib with TPA and PD98059 with TPA, respectively, for 6 h. Cells were lysed with 100 μl lysis buffer (50 mM Tris-HCl pH 8.0, 120 mM NaCl, 0.5% NP-40, 1 mM phenylmethanesulfonylfluoride). Forty micrograms of total protein were separated by 10% sodium dodecyl sulfate polyacrylamide gel electrophoresis (SDS-PAGE), were transferred to a polyvinylidene difluoride membrane (Millipore, Billerica, MA, USA), blocked with 5% nonfat milk in TBS-Tween buffer (0.12 M Tris-base, 1.5 M NaCl, and 0.1% Tween 20) for 1 h at room temperature, then were incubated with the appropriate primary antibodies, including MMP-9, VEGF, phosphorylated-ERK (p-ERK), total-ERK (T-ERK) and β-actin (Millipore) overnight at 4˚C, followed by incubation with horseradish peroxidase-conjugated secondary antibodies for 30 min at room temperature. The bound antibody was detected by enhanced chemiluminescence (ECL; Millipore). The ImageJ software (National

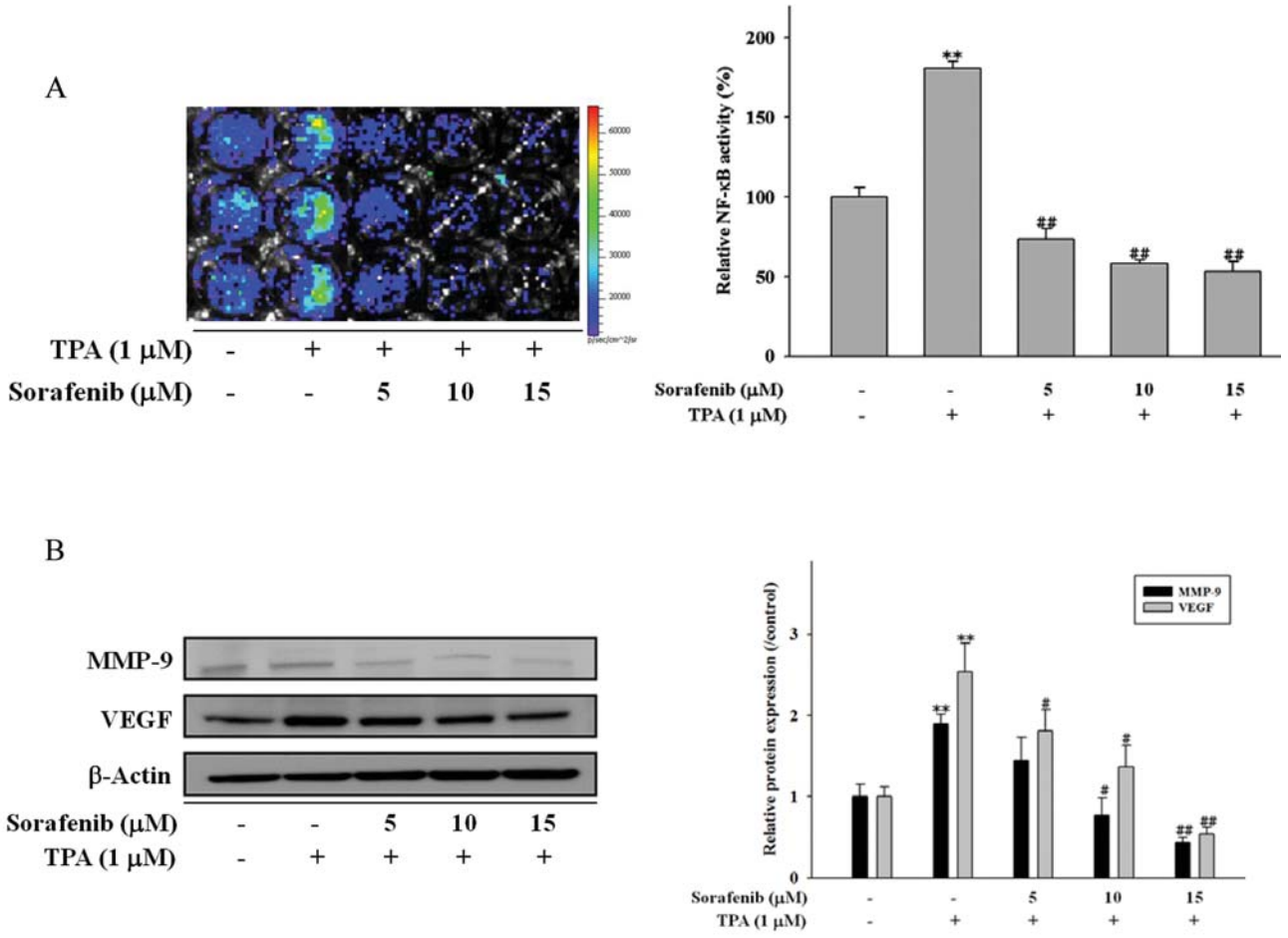

Figure 4. *12-O-Tetradecanoylphorbol-13-acetate (TPA)-induced nuclear factor kappaB (NF-κB) activity, matrix metalloproteinase-9 (MMP-9) and vascular endothelial growth factor (VEGF) overexpressions are inhibited by sorafenib in Huh7/NF-κB-luc2 cells. Cells were treated with dimethyl sulfoxide (DMSO) and sorafenib 30 min prior to the addition of TPA, respectively, and cultured for another 6 hours. A: Top: Bioluminescent imaging (BLI) of the relative NF-κB activity; bottom: quantification of the relative NF-κB activity. B: Top: Western blotting of MMP-9 and VEGF expressions using β-actin as the internal control; bottom: quantification of the western blotting. Data are presented as means±SD (n=3). **p<0.01 as compared with that of DMSO-treated control; #p<0.05, ##p<0.01 as compared with that of TPA-treated group. The experiments were repeated three times.*

Institutes of Health, Bethesda, Maryland, USA) was used for the quantitative analysis, and the protein expressions of the treated groups were compared against those of the DMSO-treated control.

Electrophoretic mobility shift assay (EMSA). Cells were treated similarly, as described for western blotting. DNA/NF-κB binding was analyzed with an EMSA kit (Pierce, Rockford, IL, USA). Nuclear fractions of Huh7/NF-κB-*luc2* cells were isolated using the Nuclear Extraction Kit (Chemicon International). The isolation and analysis procedures followed the protocols provided by the manufacturer. The following DNA sequences were synthesized for EMSA analysis. Sense: AGTTGAGGGGACTTTCCCAGGC; antisense: GCCTGGG AAAGTCCCCTCAAC. The NF-κB/DNA binding activity was evaluated using the LightShift Chemiluminescent EMSA kit (Pierce). Nuclear extracts were incubated with the biotin-labeled DNA probe for 20 min at room temperature. The DNA/protein complex was separated from the free oligonucleotides on a 10% polyacrylamide gel, was transferred to a nylon membrane and cross-linked by UV light. The membrane was incubated with streptavidin-horseradish peroxidase, and detected by ECL (Pierce). The ImageJ software was used for the quantitative analysis, and the NF-κB/DNA binding activities of treated groups were compared with those of the DMSO-treated control.

Reverse transcription polymerase chain reaction (RT-PCR) analysis. Huh7/NF-κB-luc2 cells 2×10^6 were seeded into 100-mm diameter dishes for 24 h before treatment. Six h post treatment with TPA, total RNA extraction was performed with a commercialized kit (NucleoSpin®; Macherey-Nagel, Düren, North Rhine-Westphalia, Germany), and the concentration of total RNA was determined. RNA, 1 μg was converted to cDNA with a RT-PCR kit (Epicentre Biotechnologies, Madison, WI, USA), according to the manufacturer's instruction. The primer sequences used were: 5'-CCCGGACCAAGGATACAG-3' (sense), and 5'-GGCTTTCTCT CGGTACTG-3' (antisense) for *MMP-9*; 5'-AATCGAGACCCTG

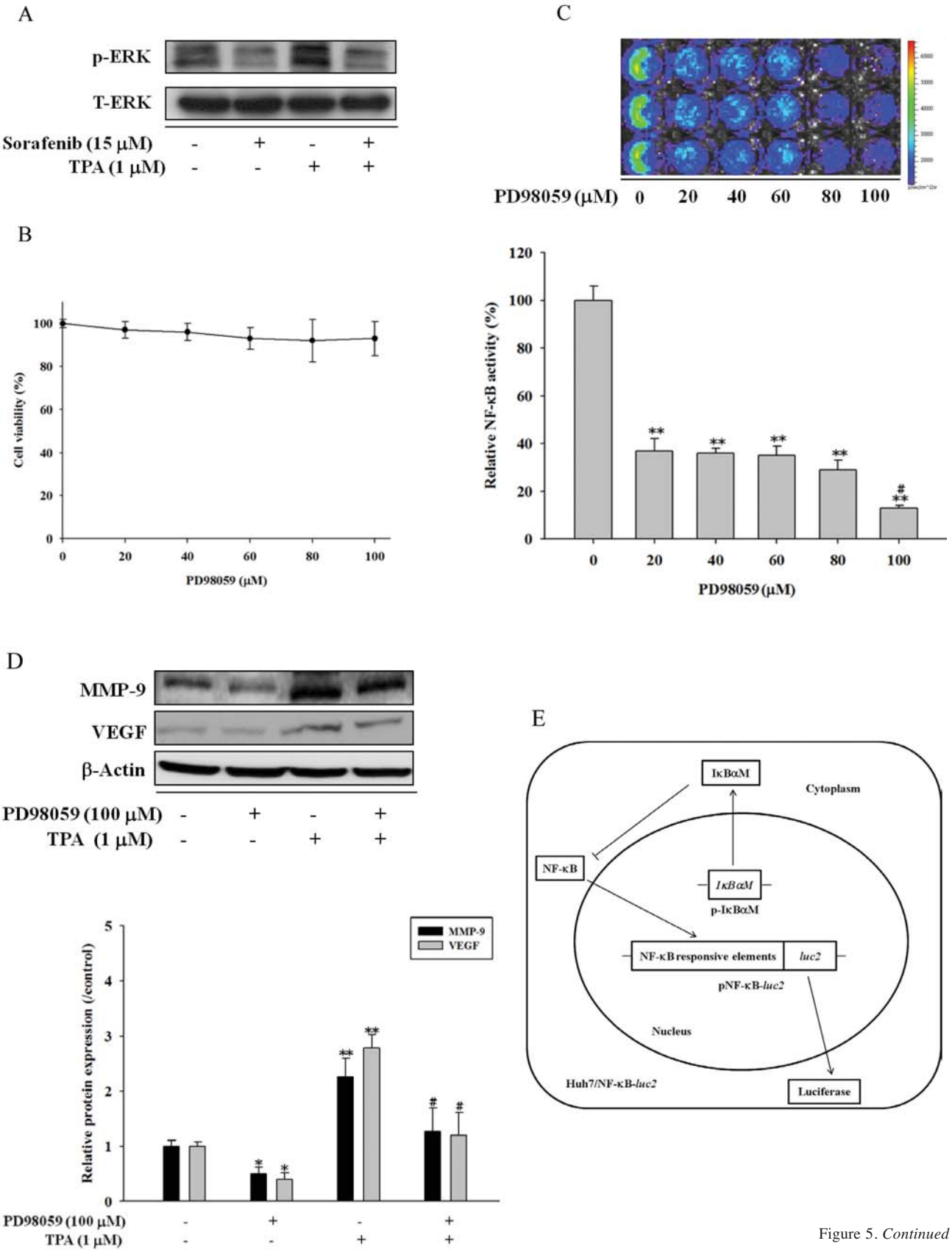

Figure 5. *Continued*

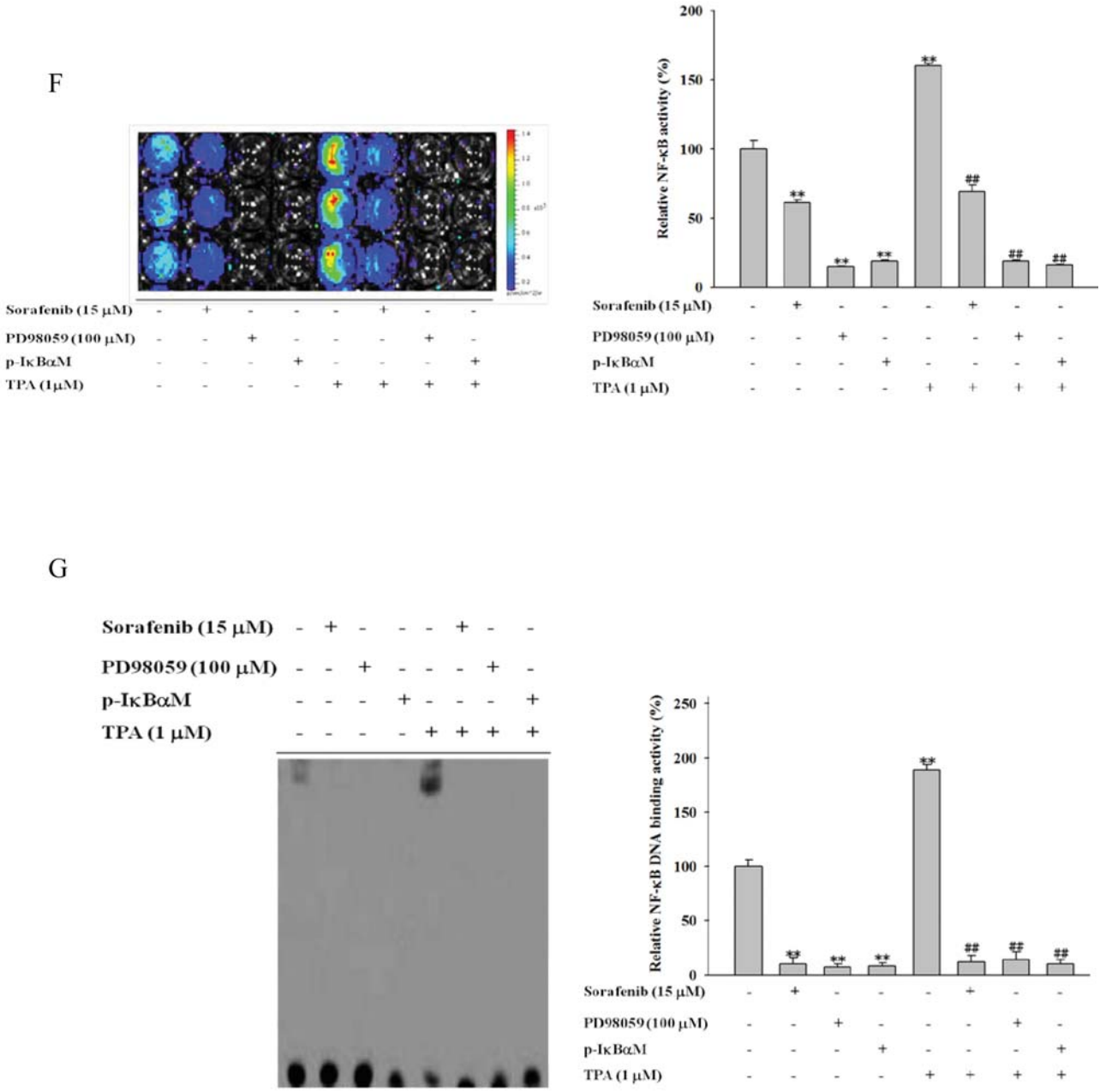

Figure 5. *12-O-Tetradecanoylphorbol-13-acetate (TPA)-induced nuclear factor kappaB (NF-κB) activity, matrix metalloproteinase-9 (MMP-9) and vascular endothelial growth factor (VEGF) expressions suppressed by sorafenib in Huh7/NF-κB-luc2 cells via the suppression of extracellular signal-regulated kinase (ERK) signal pathway. Cells were treated with dimethyl sulfoxide (DMSO), sorafenib, and PD98059 30 minutes prior to the addition of TPA, respectively, and incubated for another 6 hours. A: TPA-induced ERK phosphorylation is inhibited by sorafenib. B: No cytotoxicity was found in cells treated with various concentrations of PD98059 for 6 hours. C: Intrinsic NF-κB activity is inhibited by the treatment with PD98059 for 6 hours. Top: Bioluminescent imaging (BLI) of the relative NF-κB activity; bottom: quantification of BLI. D: Intrinsic and TPA-induced MMP-9 and VEGF expressions are suppressed by PD98059. Top: Western blotting; bottom: quantification of the western blotting. E: Inhibitor of kappaB-α mutant vector (p-IκBαM), a super repressor of NF-κB, bound to NF-κB with high affinity, preventing its phosphorylation by inhibitor of kappaB kinase (IKK). As a consequence, NF-κB is sequestered in the cytoplasm. F: Intrinsic and TPA-induced NF-κB activities are decreased in cells treated with sorafenib, PD98059, and transfection with p-IκBαM, respectively. Top: BLI of the relative NF-κB activity; bottom: quantification of BLI. G: Intrinsic and TPA-induced NF-κB/DNA binding activities are blocked in cells treated with sorafenib, PD98059, and transfection with p-IκBαM, respectively. Top: NF-κB/DNA binding activity as determined by EMSA; bottom: quantification of EMSA. Data are presented as means±SD (n=3). *p<0.05, **p<0.01 as compared with that of DMSO-treated control; #p<0.05, ##p<0.01 as compared with that of TPA-treated only group. The experiments were repeated three times.*

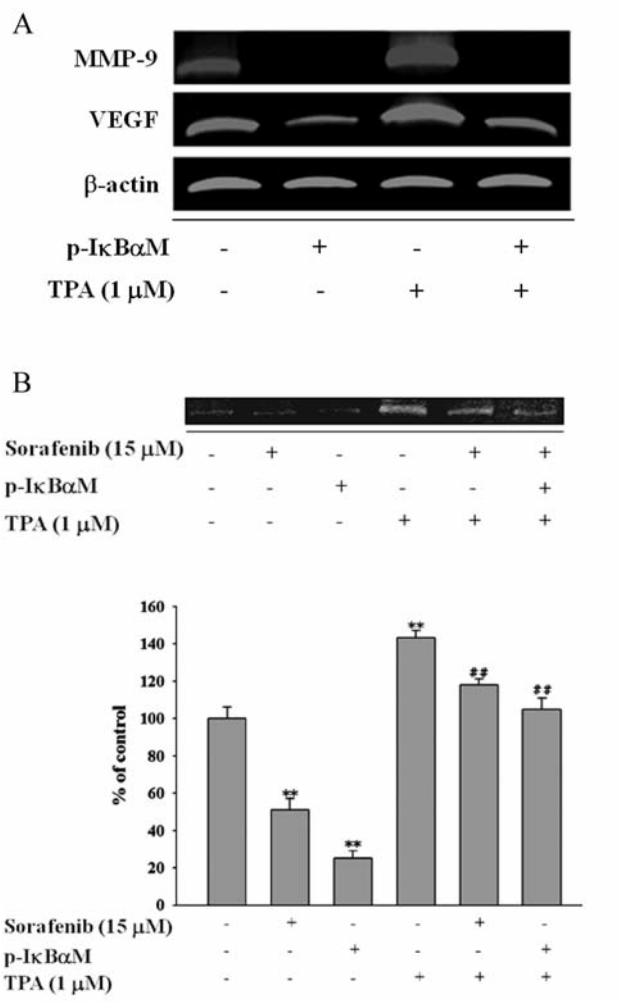

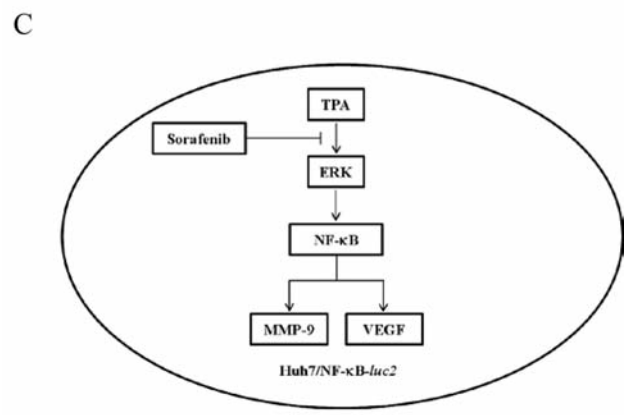

Figure 6. *Blockade of nuclear factor kappaB (NF-κB) activity results in the decrease of 12-O-tetradecanoylphorbol-13-acetate (TPA)-induced matrix metalloproteinase-9 (MMP-9) and vascular endothelial growth factor (VEGF) expressions, and the secretion of MMP-9 into the cultured medium of Huh7/NF-κB-luc2 cells. Cells were treated with sorafenib and inhibitor of kappaB-α mutant vector (p-IκBαM) 30 minutes prior to the addition of TPA, and incubated for another 6 hours. A: The mRNA expressions of MMP-9, VEGF, and β-actin were assayed with RT-PCR. B: Top: the MMP-9 protein released into the cultured medium was analyzed with gelatin zymography; bottom: quantification of the top panel. Data are presented as means±SD (n=3). **p<0.01 as compared with that of dimethyl sulfoxide (DMSO)-treated control; ##p<0.01 as compared with that of TPA-treated only group. The experiments were repeated three times. C: The suggested mechanism for TPA-induced MMP-9 and VEGF expressions inhibited by sorafenib through extracellular signal-regulated kinase (ERK)/NF-κB pathway.*

GTGGACA-3' (sense), and 5'-TTAACTCAAGCTGCCTCGCC-3' (antisense) for *VEGF*; 5'-GCGGGAAATCGTGCGTGACATT3' (sense), and 5'-GATGGAGTTGAAGGTAGTTTCGTG-3' (antisense) for β-actin. The conditions for MMP-9 and β-actin PCR were the following. One cycle of initial denaturation for 5 min at 94˚C was followed by 30 and 21 cycles of amplification for MMP-9 and β-actin, respectively. The amplification cycle consists of 1 min at 94˚C, 1 min at 60˚C, and 1 min at 72˚C. The last step was one cycle of final extension for 10 min at 72˚C. For PCR of *VEGF*, the protocol consisted of an initial denaturation for 2 min at 95˚C, followed by amplification for 30 cycles (95˚C for 1 min, 53˚C for 1 min, and 68˚C for 2 min) and a final extension step for 10 min at 68˚C. The PCR product was analyzed by electrophoresis in a 1.5% agarose gel and stained with ethidium bromide.

Gelatin zymography assay. Polyacrylamide gels, 10%, containing 0.1% gelatin were prepared for zymography. Culture media were resuspended in sample buffer (0.125 M Tris-Hcl, 20% glycerol, 10% SDS, 72 μM bromophenol blue) and run on the 10% polyacrylamide gel. After electrophoresis, gels were washed with buffer (2.5% Triton X-100) on a shaker for 30 min at room temperature, to remove SDS. The gels were then incubated in an incubation buffer (50 mM Tris–HCl, 5mM $CaCl_2$, 0.15M NaCl, and 1% Triton X-100) for 48 h at 37˚C. The gels were subsequently stained with Coomassie blue G-250 and destained in a solution composed of 30% methanol and 10% acetic acid to detect MMP-9 secretion.

Statistics. Statistical analysis was determined either by one-sample *t*-test, when compared with the DMSO-treated control or by the Student's *t*-test when compared with the TPA-treated group. Data are shown with means±standard deviations.

Results

Effects of sorafenib on Huh7/NF-κB-luc2 cell viability. The cytotoxicity of sorafenib on Huh7/NF-κB-*luc2* cells was determined by the MTT assay. Figure 1 shows that the cell viability was reduced by 14-33% compared to that of the control, after treatment with different concentrations of sorafenib for 24 h ($p<0.01$). Notably, no obvious cytotoxicity was found when cells were treated with 5-15 μM sorafenib for 6 h.

Sorafenib reduces NF-κB activity, MMP-9 and VEGF expression. The effect of sorafenib on NF-κB activity was evaluated with luciferase reporter gene assay. Huh7/NF-κB-

luc2 cells were treated with 0, 5, 10, and 15 μM sorafenib for 6 h. Figure 2A shows that the relative NF-κB activity of the cells was inhibited by sorafenib in a dose-dependent manner, with 20-45% reduction compared to that of the control ($p<0.01$). In addition, the effects of sorafenib on MMP-9 and VEGF expressions were evaluated with western blotting. Figure 2B shows that relative protein levels of MMP-9 and VEGF were also inhibited in a dose-dependent manner, by 30-80% compared to those of the control ($p<0.01$).

NF-κB activity, MMP-9 and VEGF expressions are induced by TPA. Huh7/NF-κB-*luc2* cells were treated with 0-1 μM TPA for 6 h. Figure 3A shows that the NF-κB activity in the luciferase reporter gene assay was increased in a dose-dependent manner, by 30-75% compared to that of the control ($p<0.05$). In addition, the relative protein levels of MMP-9 and VEGF were also increased by 0.5-1.5-fold compared to those of the control ($p<0.05$), as shown in Figure 3B.

Sorafenib suppresses TPA-induced NF-κB activity, MMP-9 and VEGF overexpressions. Huh7/NF-κB-*luc2* cells were treated with 1 μM TPA alone, and 0-15 μM sorafenib 30 min prior to the addition of 1 μM TPA, respectively, and were incubated for another 6 h. The relative NF-κB activity increased, following TPA treatment by 80%, compared to that of the control. Notably, sorafenib reduced TPA-induced relative NF-κB activity by 60-75% compared to that of the TPA-treated group (Figure 4A, $p<0.01$). Moreover, Figure 4B shows that overexpression of MMP-9 and VEGF, induced by TPA, are inhibited by sorafenib. The relative protein expressions of MMP-9 and VEGF following TPA treatment were increased by 0.8- and 1.5-fold compared to that of the control as shown in Figure 4B ($p<0.01$). Notably, the overexpression of MMP-9 and VEGF, induced by TPA, was also suppressed by the pretreatment with sorafenib ($p<0.05$).

Sorafenib inhibits TPA-induced NF-κB activity, MMP-9 and VEGF overexpression via suppression of ERK phosphorylation. To determine the regulatory mechanism of sorafenib on TPA-induced NF-κB activity, Huh7/NF-κB-*luc2* cells were treated with 15 μM sorafenib and 100 μM PD98059, an ERK inhibitor, 30 min prior to the addition of 1 μM TPA, respectively, and incubated for another 6 h. Figure 5A shows that ERK phosphorylation was increased in Huh7/NF-κB-*luc2* cells after treatment with TPA alone. The induction, however, was inhibited by pretreatment with 15 μM sorafenib. On the other hand, the cell viability was not significantly changed when cells were treated with 0-100 μM PD98059 for 6 h (Figure 5B). PD98059 significantly reduced intrinsic and TPA-induced relative NF-κB activity, MMP-9 and VEGF expression (Figures 5C and 5D), in a pattern similar to the effects of sorafenib. Huh7/NF-κB-*luc2* cell line was also co-transfected with p-IκBαM super repressor to sequester NF-κB in the cytoplasm (28), as a negative control (Figure 5E). Figure 5F shows that both sorafenib and PD98059 significantly suppressed intrinsic and TPA-induced relative NF-κB activity ($p<0.01$). Intrinsic and TPA-induced NF-κB/DNA binding activity assayed by EMSA was reduced by sorafenib treatment as shown in Figure 5G.

Sorafenib and p-IκBαM reduces TPA-induced MMP-9 and VEGF overexpression, and MMP-9 activity. To evaluate the role that NF-κB signaling pathway plays in TPA-induced *MMP-9* and *VEGF* expressions, RT-PCR was used to analyze the mRNA levels of both genes. Huh7/NF-κB-*luc2* cells were transfected with p-IκBαM prior to the addition of 1 μM TPA, and were incubated for 6 h. Figure 6A shows that TPA-induced *MMP-9* and *VEGF* mRNA levels, were reduced in the cells transfected with p-IκBαM. Furthermore, the effect of p-IκBαM or sorafenib on intrinsic and TPA-induced MMP-9 secretion in the cultured medium, was assayed with gelatin zymography. Figure 6B shows that TPA-induced MMP-9 secretion of Huh7/NF-κB-*luc2* cells was reduced when cells were transfected with p-IκBαM or pre-treated with 15 μM sorafenib for 30 min prior to the addition of 1 μM TPA.

Discussion

How sorafenib exerts its inhibitory action on tumor metastasis and angiogenesis in HCC has not been completely elucidated. In this study, we used TPA, a potent tumor promoter, to induce the MMP-9 and VEGF expression, in order to elucidate the effect of sorafenib on the NF-κB activity and its correlation with these two proteins in HCC. We found that the inhibition of TPA-induced MMP-9 and VEGF expression by sorafenib occurred *via* the ERK/NF-κB pathway. This finding may implicate the potential application for sorafenib as an NF-κB inhibitor to reduce metastasis and invasiveness of human HCC.

Activation of NF-κB is a common and early event found in human HCC, caused by viral or nonviral factors, and has also been associated with the acquisition of a transformed phenotype during hepatocarcinogenesis (10). Many NF-κB-regulated down-stream gene products, such as B-cell lymphoma-extra large (BCL-xL), cyclin D1, MMP-9, VEGF, and cyclooxygenase-2 (COX-2), contribute to the tumor progression and invasion in HCC (12, 29). Angiogenic and metastatic signaling pathway through the RAS/RAF/MEK/ERK cascade has been shown not only to be involved in the development of HCC, but also in the regulation of cell proliferation, apoptosis, cytokine expression and production of MMPs and VEGF in HCC (30, 31). Several studies have reported that phosphorylation of AKT is not affected by sorafenib treatment in HCC, and TPA-induced invasion and migration occurs through activation of the protein kinase C (PKC)-α/ERK/NF-κB pathway in glioblastoma cells (20, 23). Although phosphatidylinositol-3-kinase (PI3K)/AKT pathway

and RAS/RAF/MEK/ERK signaling pathway are involved in the NF-κB activation of various cancer cell types (32, 33), the regulatory effect of sorafenib on the ERK/NF-κB pathway in HCC remains unclear.

The antitumor effects of sorafenib take place through the inhibition of RAF kinase and down-stream ERK phosphorylation and may also be attributed to the inhibition of receptor tyrosine kinase function of VEGFR and PDGFR, resulting in suppression of tumor proliferation and angiogenesis (18-20). Sorafenib also inhibits growth factor-induced cell migration *via* down-regulation of MMP-9 expression in HCC (34). Here, Huh7/NF-κB-*luc2* cells were treated with 5-15 μM sorafenib for 6 h to clarify the regulatory effect of sorafenib on the ERK/NF-κB pathway, since the cell viability was not significantly changed as compared with that of the control (Figure 1). Therefore, the decrease in protein expression after 6-hour sorafenib treatment appears to be due to the change in signal transduction rather than the cell death. This may also apply for HCC cells treated with PD98059 (Figure 5B). The concentrations of 15 μM sorafenib and 100 μM PD98059 were used in this study since the maximal suppression of NF-κB activity was found under these conditions (Figure 2A and 5C). Intrinsic NF-κB activity and down-stream effector proteins, such as MMP-9 and VEGF, were suppressed by sorafenib, but were induced by TPA (Figure 2 and 3). Nevertheless, TPA-induced NF-κB activity, MMP-9 and VEGF overexpression were still suppressed by sorafenib (Figure 4). Notably, TPA-induced ERK phosphorylation was inhibited by sorafenib (Figure 5A). Cells pre-treated with 5-15 μM sorafenib and 100 μM PD98059 (ERK inhibitor), respectively, prior to the treatment of 1 μM TPA, had reduced TPA-induced NF-κB activity, MMP-9 and VEGF overexpressions as well (Figure 5D and 5F). On this basis, we suggest that the suppression of the NF-κB activation, and MMP-9 and VEGF expressions by sorafenib occur through the inhibition of ERK phosphorylation. However, the effects of sorafenib on the NF-κB pathway in HCC may be different in other cancer cell lines. It has been shown that sorafenib-down-regulated expression of anti-apoptotic proteins, such as myeloid leukemia cell differentiation protein-1 (MCL-1) and cellular inhibitor of apoptosis protein 2 (cIAP2), takes place *via* the inhibition of tumor necrosis factor α (TNFα)-related apoptosis-inducing ligand (TRAIL)-induced NF-κB activation in human colorectal cancer cells (35). On the contrary, NF-κB activation in pancreatic cancer stem cells, induced by sorafenib, may lead to the induction of epithelial mesenchymal transition, resulting in the selection of a more invasive phenotype among pancreatic cancer cells (36). In this study, we found that sorafenib suppressed TPA-induced NF-κB/DNA binding activity with similar efficacy, as shown with PD98059 and p-IκBαM transfection (Figure 5G). Consequently, the suppression of NF-κB pathway leads to the reduced transcription of *MMP-9* and *VEGF* mRNA (Figure 6A) and of subsequent protein expressions, as shown in Figure 4B. Decreased MMP-9 enzyme activity by sorafenib and p-IκBαM transfection, assayed by zymography (Figure 6B and 6C), suggests that inhibition of NF-κB pathway may reduce the invasion of HCC cells. Furthermore, TPA-induced MMP-9 and VEGF expressions suppressed by sorafenib *via* the ERK/NF-κB pathway (Figure 6C), also suggest that NF-κB may be a potential target for HCC treatment.

Sorafenib suppresses the ERK/NF-κB signaling pathways, and is an effective inhibitor of TPA-induced MMP-9 and VEGF expression in human HCC cells. The ERK/NF-κB pathway implicates the mechanistic link to the therapeutic efficacy of sorafenib, to reduce the invasive capability of HCC cells. Therefore, sorafenib may be a promising ingredient for multi-modality anticancer treatments through inhibition of metastasis and angiogenesis in patients with HCC.

Acknowledgements

This study was supported by grants NSC99-2623-E-010-001-NU and 100-NU-E-010-003-NU from the National Science Council, Taipei, Taiwan. No conflict of interest is declared by any of the Authors. We thank Molecular and Genetic Imaging Core (MAGIC)/NRPGM, Taiwan for the support of the imaging facilities.

References

1 Ferlay J, Shin HR, Bray F, Forman D, Mathers C and Parkin DM: Cancer Incidence and Mortality Worldwide: IARC CancerBase No. 10. Ver.1.2: http://globocan.iarc.fr. Accessed 29th, January, 2012.

2 Poon RT and Fan ST: Hepatectomy for hepatocellular carcinoma: patient selection and postoperative outcome. Liver Transpl *10*: S39-45, 2004.

3 Comoglio PM and Trusolino L: Invasive growth: from development to metastasis. J Clin Invest *109*: 857-862, 2002.

4 Coussens LM and Werb Z: Matrix metalloproteinases and the development of cancer. Chem Biol *3*: 895-904, 1996.

5 Poon RT, Ng IO, Lau C, Yu WC, Yang ZF, Fan ST and Wong J: Tumor microvessel density as a predictor of recurrence after resection of hepatocellular carcinoma: a prospective study. J Clin Oncol *20*: 1775-1785, 2002.

6 Moon WS, Rhyu KH, Kang MJ, Lee DG, Yu HC, Yeum JH, Koh GY and Tarnawski AS: Overexpression of VEGF and angiopoietin 2: A key to high vascularity of hepatocellular carcinoma? Mod Pathol *16*: 552-557, 2003.

7 Pikarsky E, Porat RM, Stein I, Abramovitch R, Amit S, Kasem S, Gutkovich-Pyest E, Urieli-Shoval S, Galun E and Ben-Neriah Y: NF-kappaB functions as a tumour promoter in inflammation-associated cancer. Nature *431*: 461-466, 2004.

8 El-Serag HB: Hepatocellular Carcinoma. N Engl J Med *365*: 1118-1127, 2011.

9 Karin M: Nuclear factor-kappaB in cancer development and progression. Nature *441*: 431-436, 2006.

10 Luedde T and Schwabe RF: NF-kappaB in the liver – linking injury, fibrosis and hepatocellular carcinoma. Nat Rev Gastroenterol Hepatol *8*: 108-118, 2011.

11 Maeda S, Kamata H, Luo JL, Leffert H and Karin M: IKKbeta couples hepatocyte death to cytokine-driven compensatory proliferation that promotes chemical hepatocarcinogenesis. Cell *121*: 977-990, 2005.
12 Wu JM, Sheng H, Saxena R, Skill NJ, Bhat-Nakshatri P, Yu M, Nakshatri H and Maluccio MA: NF-kappaB inhibition in human hepatocellular carcinoma and its potential as adjunct to sorafenib based therapy. Cancer Lett *278*: 145-155, 2009.
13 Hah N and Lee ST: An absolute role of the PKC-dependent NF-kappaB activation for induction of MMP-9 in hepatocellular carcinoma cells. Biochem Biophys Res Commun *305*: 428-433, 2003.
14 Coussens LM and Werb Z: Inflammation and cancer. Nature *420*: 860-867, 2002.
15 Schomer-Miller B, Higashimoto T, Lee YK and Zandi E: Regulation of IkappaB kinase (IKK) complex by IKKgamma-dependent phosphorylation of the T-loop and C terminus of IKKbeta. J Biol Chem *281*: 15268-15276, 2006.
16 Liu YC, Chiang IT, Hsu FT and Hwang JJ: Using NF-κB as a molecular target for theranostics in radiation oncology research. Expert Rev Mol Diagn *12*: 139-146, 2012.
17 Calvisi DF, Ladu S, Gorden A, Farina M, Conner EA, Lee JS, Factor VM and Thorgeirsson SS: Ubiquitous activation of RAS and JAK/STAT pathways in human HCC. Gastroenterology *130*: 1117-1128, 2006.
18 Siegel AB, Olsen SK, Magun A and Brown RS Jr.: Sorafenib: Where do we go from here? Hepatology *52*: 360-369, 2010.
19 Wilhelm SM, Carter C, Tang L, Wilkie D, McNabola A, Rong H, Chen C, Zhang X, Vincent P, McHugh M, Cao Y, Shujath J, Gawlak S, Eveleigh D, Rowley B, Liu L, Adnane L, Lynch M, Auclair D, Taylor I, Gedrich R, Voznesensky A, Riedl B, Post LE, Bollag G and Trail PA: BAY 43-9006 exhibits broad-spectrum oral antitumor activity and targets the RAF/MEK/ERK pathway and receptor tyrosine kinases involved in tumor progression and angiogenesis. Cancer Res *64*: 7099-7109, 2004.
20 Liu L, Cao Y, Chen C, Zhang X, McNabola A, Wilkie D, Wilhelm S, Lynch M and Carter C: Sorafenib blocks the RAF/MEK/ERK pathway, inhibits tumor angiogenesis, and induces tumor cell apoptosis in hepatocellular carcinoma model PLC/PRF/5. Cancer Res *66*: 11851-11858, 2006.
21 Llovet JM, Ricci S, Mazzaferro V, Hilgard P, Gane E, Blanc JF, de Oliveira AC, Santoro A, Raoul JL, Forner A, Schwartz M, Porta C, Zeuzem S, Bolondi L, Greten TF, Galle PR, Seitz JF, Borbath I, Haussinger D, Giannaris T, Shan M, Moscovici M, Voliotis D and Bruix J: Sorafenib in advanced hepatocellular carcinoma. New Engl J M *359*: 378-390, 2008.
22 Arsura M, Mercurio F, Oliver AL, Thorgeirsson SS and Sonenshein GE: Role of the IkappaB kinase complex in oncogenic Ras- and Raf-mediated transformation of rat liver epithelial cells. Mol Cell Biol *20*: 5381-5391, 2000.
23 Lin CW, Shen SC, Chien CC, Yang LY, Shia LT and Chen YC: 12-*O*-Tetradecanoylphorbol-13-acetate-induced invasion/migration of glioblastoma cells through activating PKCalpha/ERK/NF-kappaB-dependent MMP-9 expression. J Cell Physiol *225*: 472-481, 2010.
24 Kim S, Choi JH, Lim HI, Lee SK, Kim WW, Kim JS, Kim JH, Choe JH, Yang JH, Nam SJ and Lee JE: Silibinin prevents TPA-induced MMP-9 expression and VEGF secretion by inactivation of the RAF/MEK/ERK pathway in MCF-7 human breast cancer cells. Phytomedicine *16*: 573-580, 2009.
25 Zhou X, Yang J, Wang Y, Li W, Li-Ling J, Deng Y and Zhang M: Cucurbitacin B inhibits 12-*O*-tetradecanoylphorbol-13-acetate-induced invasion and migration of human hepatoma cells through inactivating mitogen-activated protein kinase and PI3K/AKT signal transduction pathways. Hepatol Res *42*: 401-411, 2012.
26 Kuo YC, Lin WC, Chiang IT, Chang YF, Chen CW, Su SH, Chen CL and Hwang JJ: Sorafenib sensitizes human colorectal carcinoma to radiation *via* suppression of NF-κB expression *in vitro* and *in vivo*. Biomed Pharmacother *66*: 12-20, 2012.
27 Bankston D, Dumas J, Natero R, Riedl B, Monahan M and Sibley R: A scaleable synthesis of BAY 43-9006: A potent RAF kinase inhibitor for the treatment of cancer. Org Process Res Dev *6*: 777-781, 2002.
28 Patel NM, Nozaki S, Shortle NH, Bhat-Nakshatri P, Newton TR, Rice S, Gelfanov V, Boswell SH, Goulet RJ Jr., Sledge GW Jr. and Nakshatri H: Paclitaxel sensitivity of breast cancer cells with constitutively active NF-kappaB is enhanced by IkappaBalpha super-repressor and parthenolide. Oncogene *19*: 4159-4169, 2000.
29 Berasain C, Castillo J, Perugorria MJ, Latasa MU, Prieto J and Avila MA: Inflammation and liver cancer: new molecular links. Ann N Y Acad Sci 1155: 206-221, 2009.
30 Wiedmann MW and Mossner J: Molecular targeted therapy of hepatocellular carcinoma – results of the first clinical studies. Curr Cancer Drug Targets *11*: 714-733, 2011.
31 Mayoral R, Fernandez-Martinez A, Bosca L and Martin-Sanz P: Prostaglandin E2 promotes migration and adhesion in hepatocellular carcinoma cells. Carcinogenesis *26*: 753-761, 2005.
32 Lee YR, Noh EM, Oh HJ, Hur H, Kim JM, Han JH, Hwang JK, Park BH, Park JW, Youn HJ, Jung SH, Kim BS, Jung JY, Lee SH, Park CS and Kim JS: Dihydroavenanthramide D inhibits human breast cancer cell invasion through suppression of MMP-9 expression. Biochem Biophys Res Commun *405*: 552-557, 2011.
33 Ruhul Amin AR, Senga T, Oo ML, Thant AA and Hamaguchi M: Secretion of matrix metalloproteinase-9 by the proinflammatory cytokine, IL-1beta: a role for the dual signalling pathways, AKT and ERK. Genes Cells *8*: 515-523, 2003.
34 Feng YX, Wang T, Deng YZ, Yang P, Li JJ, Guan DX, Yao F, Zhu YQ, Qin Y, Wang H, Li N, Wu MC, Wang HY, Wang XF, Cheng SQ and Xie D: Sorafenib suppresses postsurgical recurrence and metastasis of hepatocellular carcinoma in an orthotopic mouse model. Hepatology *53*: 483-492, 2011.
35 Ricci MS, Kim SH, Ogi K, Plastaras JP, Ling J, Wang W, Jin Z, Liu YY, Dicker DT, Chiao PJ, Flaherty KT, Smith CD and El-Deiry WS: Reduction of TRAIL-induced MCL-1 and cIAP2 by c-MYC or sorafenib sensitizes resistant human cancer cells to TRAIL-induced death. Cancer Cell *12*: 66-80, 2007.
36 Rausch V, Liu L, Kallifatidis G, Baumann B, Mattern J, Gladkich J, Wirth T, Schemmer P, Buchler MW, Zoller M, Salnikov AV and Herr I: Synergistic activity of sorafenib and sulforaphane abolishes pancreatic cancer stem cell characteristics. Cancer Res *70*: 5004-5013, 2010.

Received March 27, 2012
Revised April 23, 2012
Accepted April 25, 2012